



Wavelet-based adaptive large-eddy simulation with explicit filtering



Giuliano De Stefano^a, Oleg V. Vasilyev^{b,*}

^a *Dipartimento di Ingegneria Aerospaziale e Meccanica, Seconda Università di Napoli, Italy*

^b *Department of Mechanical Engineering, University of Colorado, 427 UCB, Boulder, CO 80309, USA*

ARTICLE INFO

Article history:

Received 19 November 2011

Received in revised form 19 September 2012

Accepted 24 September 2012

Available online 16 October 2012

Keywords:

Turbulent flows

Coherent structures

Wavelets

Adaptive large eddy simulation

Explicit filtering

ABSTRACT

Stochastic coherent adaptive large-eddy simulation is a novel approach to the numerical simulation of turbulence, where the coherent energetic eddies are solved for, while modeling the influence of the less energetic coherent/incoherent background flow. The formal separation between resolved and unresolved field is obtained by wavelet threshold filtering that is inherent to the adaptive wavelet collocation numerical method. A new explicit wavelet filtering strategy is introduced and tested, by considering two different filtering levels: the physical level, which controls the turbulence model, and the numerical level that is responsible for the accuracy of numerical simulations. The theoretical basis for wavelet-based adaptive large-eddy simulation with explicit filtering and consistent dynamic modeling is given. Numerical experiments are presented for unsteady homogeneous turbulence, demonstrating the existence of grid-independent solutions.

© 2012 Elsevier Inc. All rights reserved.

1. Introduction

The stochastic coherent adaptive large-eddy simulation (SCALES) method is a novel approach to the numerical simulation of turbulent flows, where the more energetic coherent eddies are solved for, while discarding the dynamics of the less energetic background flow [1]. The decomposition of turbulence into resolved coherent and residual coherent/incoherent motions is obtained through the application of wavelet threshold filtering (WTF). The space–time evolution of the coherent velocity field is governed by the wavelet-filtered Navier–Stokes equations, where, similarly to any other large-eddy simulation (LES) approach, the effect of the unknown residual stresses is modeled.

In order to solve the SCALES governing equations in a computationally efficient manner, the adaptive wavelet collocation method (AWCM) is used, e.g. [2]. The method is a variable high-order finite-difference numerical simulation that exploits the same wavelet filtering procedure to automatically adapt the computational grid to the solution, in both location and scale. The choice of a wavelet thresholding level for the grid adaptation automatically introduces a formal separation between eddies that are resolved by the wavelet collocation grid and unresolvable sub-grid eddies. Up to now, the filtering effect induced by the use of the AWCM has been used to define the filtered-velocity in the SCALES approach, without distinguishing between physical (model) filtering and numerical filtering that is related to truncation of wavelet basis and corresponding computational mesh. Thus, there has been no practical reason, so far, to discern between explicit and implicit wavelet-filtering. Along this line, the residual stresses have been referred to and treated as subgrid-scale (SGS) stresses, e.g. [3,4].

The implicit approach makes it impossible to separate between filtering, modeling and numerical issues. This is a fundamental problem in LES methods [5] that becomes even more important in the wavelet-based formulation, where the numerical solver allows for the automatic mesh refinement in flow regions with inadequate modeled dissipation.

* Corresponding author. Tel.: +1 303 492 4717.

E-mail addresses: giuliano.destefano@unina2.it (G. De Stefano), Oleg.Vasilyev@Colorado.EDU (O.V. Vasilyev).

Furthermore, SCALES method with implicit filtering is particularly sensitive to numerical errors since the choice of a relatively high thresholding level unavoidably affects the accuracy of the AWCM-based solution.

In this work, following a strategy that is sometimes adopted in classical non-adaptive LES, e.g. [6,7], a new wavelet-based adaptive LES method with explicit filtering is introduced and tested. Two different filtering levels are considered: the physical level, which controls the level of turbulence model, and the numerical level that is solely responsible for the accuracy of calculations. The superposition of explicit filtering allows to practically control the computational errors, while keeping apart the filtering and the numerical issues.

The theoretical basis for SCALES with explicit filtering is given and numerical experiments are carried out for freely decaying homogeneous incompressible turbulence. The use of explicit wavelet filtering is studied in order to address the potential of the method to obtain grid-independent numerical solutions, as found for classical LES [8].

In the next section, the wavelet-based adaptive LES approach is briefly reviewed. The new explicit filtering SCALES method is introduced in Section 3, along with the consistent dynamic procedure for modeling the residual stresses. In Section 4, the numerical experiments are presented and discussed. Finally, in Section 5, some concluding remarks are made.

2. Wavelet-based adaptive large-eddy simulation

Different numerical methods for solving the Navier–Stokes equations in adaptive wavelet bases have been recently developed, by exploiting the efficient wavelet decomposition of turbulence into space-scale contributions, e.g. [9–12]. In the following, the wavelet-based LES approach is concisely reviewed, along with the dynamic procedure for modeling the effect of residual motions.

2.1. Wavelet-filtered velocity

In the wavelet-based adaptive LES approach, the turbulent velocity field is decomposed into two different parts: a coherent more energetic velocity field and a residual less energetic coherent/incoherent one. WTF is performed by applying the wavelet-transform to the unfiltered field, zeroing the wavelet coefficients below a given threshold, say, ϵ , and transforming back to the physical space [1]. Formally, the wavelet-filtered velocity, $\bar{u}_i^{>\epsilon}(\mathbf{x})$, is defined by expressing the instantaneous velocity field in terms of wavelet basis functions and retaining only significant wavelets, e.g. [13]:

$$\bar{u}_i^{>\epsilon}(\mathbf{x}) = \sum_{\mathbf{l} \in \mathcal{L}^0} c_{\mathbf{l}}^0 \phi_{\mathbf{l}}^0(\mathbf{x}) + \sum_{j=0}^{+\infty} \sum_{\mu=1}^{2^n-1} \sum_{\mathbf{k} \in \mathcal{K}^{\mu,j}} d_{\mathbf{k}}^{\mu,j} \psi_{\mathbf{k}}^{\mu,j}(\mathbf{x}). \quad (1)$$

$$|d_{\mathbf{k}}^{\mu,j}| > \epsilon \|u_i\|_{\text{WTF}}$$

In the above decomposition, bold subscripts denote n -dimensional indexes, while \mathcal{L}^0 and $\mathcal{K}^{\mu,j}$ are n -dimensional index sets associated with scaling functions at zero level of resolution ($\phi_{\mathbf{l}}^0$) and wavelets of family μ and level j ($\psi_{\mathbf{k}}^{\mu,j}$), respectively. Each level of resolution j consists of a family of wavelets $\psi_{\mathbf{k}}^{\mu,j}$ having the same scale but located at different grid positions.

Thus, the turbulent velocity field results decomposed as $u_i = \bar{u}_i^{>\epsilon} + u'_i$, where $\bar{u}_i^{>\epsilon}$ stands for the wavelet-filtered velocity at level ϵ , while u'_i corresponds to the background less energetic flow. Depending on the choice of the WTF level that is dictated by the desired turbulence resolution, only a relatively small number of wavelets are retained in representing the filtered field $\bar{u}_i^{>\epsilon}$. It can be shown that the relative difference between unfiltered and filtered velocity is bounded by the thresholding level ϵ [14].

The high compression property of the wavelet-based decomposition is illustrated in Table 1, where the percentage of active wavelets and retained energy/enstrophy are reported as a function of the WTF level ϵ , for a given turbulent velocity field. The latter corresponds to an instantaneous realization of statistically stationary homogeneous turbulence at $Re_\lambda \cong 120$ (λ being the Taylor microscale) provided by a pseudo-spectral DNS calculation [15]. For instance, by retaining less than 1% of the 512^3 available wavelets, one is able to capture more than 99% of the total energy and almost 90% of the total enstrophy of the flow (as it happens for $\epsilon = 0.25$).

For a given level of turbulence resolution, the fraction of enstrophy that is resolved is lower than the energy fraction because the small dissipative scales are partially filtered out. However, differently from classical low-pass filtering used in non-adaptive LES, the small scale turbulence is partly represented by the wavelet-filtered field. In fact, one of the distinctive features of WTF stands in the ability to capture energetic coherent eddies of any size. This is particularly evident

Table 1
Percentage of active wavelets and retained energy/enstrophy for different WTF levels.

Level ϵ	Wavelets (%)	Energy (%)	Enstrophy (%)
0.45	0.11	97.8	66.0
0.35	0.26	99.0	78.4
0.25	0.61	99.5	87.0
0.15	1.86	99.9	95.1

by inspection of energy and enstrophy spectra, as reported in previous studies, e.g. [9,16], and confirmed by the present results.

2.2. Wavelet-filtered Navier–Stokes equations

For incompressible turbulent flows, the space–time evolution of the wavelet-filtered velocity is governed by the following wavelet-filtered continuity and Navier–Stokes equations:

$$\frac{\partial \bar{u}_i^{>\epsilon}}{\partial x_i} = 0, \quad (2)$$

$$\frac{\partial \bar{u}_i^{>\epsilon}}{\partial t} + \frac{\partial \bar{u}_i^{>\epsilon} \bar{u}_j^{>\epsilon}}{\partial x_j} = -\frac{1}{\rho} \frac{\partial \bar{p}^{>\epsilon}}{\partial x_i} + \nu \frac{\partial^2 \bar{u}_i^{>\epsilon}}{\partial x_j \partial x_j} - \frac{\partial \tau_{ij}}{\partial x_j}, \quad (3)$$

where ρ and ν are the constant density and kinematic viscosity of the fluid. The bar symbol in the notation of the pressure variable, $\bar{p}^{>\epsilon}$, does not imply the application of WTF, but is used for consistency with the other terms. Actually, the pressure term in the filtered momentum Eq. (3) must be viewed as a Lagrange multiplier enforcing the incompressibility constraint (2).

As in any LES approach, the filtered momentum equation appears in unclosed form and a closure model for the unknown residual-stress tensor

$$\tau_{ij} = \overline{u_i u_j^{>\epsilon}} - \bar{u}_i^{>\epsilon} \bar{u}_j^{>\epsilon}, \quad (4)$$

must be introduced. The main aim of the model is to provide adequate energy dissipation that mimics the net effect of unresolved eddies on the dynamics of the resolved ones. In absence of any turbulence forcing, the kinetic-energy of the wavelet-filtered velocity field $\langle \frac{1}{2} \bar{u}_i^{>\epsilon} \bar{u}_i^{>\epsilon} \rangle$ decays in time, owing to the combined action of resolved viscous dissipation $\langle 2\nu \bar{S}_{ij}^{>\epsilon} \bar{S}_{ij}^{>\epsilon} \rangle$ and unresolved residual-stress dissipation $\langle -\tau_{ij} \bar{S}_{ij}^{>\epsilon} \rangle$, where $\bar{S}_{ij}^{>\epsilon} = 1/2(\partial \bar{u}_i^{>\epsilon} / \partial x_j + \partial \bar{u}_j^{>\epsilon} / \partial x_i)$ stands for the resolved wavelet-filtered rate-of-strain tensor, with angular brackets denoting volume-averaged quantities.

In practice, a model for the anisotropic part of the residual-stress tensor $\tau_{ij}^* \equiv \tau_{ij} - (\tau_{kk}/3)\delta_{ij}$ is considered, while the isotropic part is included in the wavelet-filtered pressure variable that is resolved. For this reason, the energy dissipation associated with the deviatoric residual stresses, $\Pi \equiv \langle -\tau_{ij}^* \bar{S}_{ij}^{>\epsilon} \rangle$, must be approximated.

From the mathematical point of view, once the residual-stress tensor is given as a function of the resolved velocity $\bar{u}_i^{>\epsilon}$ and suitable initial conditions are provided, the above SCALES governing equations can be solved using any numerical method. In practice, they are solved using the adaptive wavelet collocation method, where the same WTF procedure is exploited to automatically adapt the computational grid to the numerical solution, in both location and scale, e.g. [2]. The use of the AWCM procedure involves an inevitable built-in filtering effect associated to the wavelet threshold that is used to control the numerical accuracy, say, ϵ_g .

Until now all SCALES studies have been conducted using the implicit filtering operation induced by the wavelet basis truncation/adaptive computational grid. In other words, the wavelet-filtered velocity has been defined by simply assuming $\epsilon = \epsilon_g$, without performing any explicit filtering operation that could be related to the use of smaller numerical wavelet thresholds. This way, the residual stresses (4) have been viewed and modeled as SGS stresses. This simple approach, however, introduces an inherent unavoidable connection between the turbulence resolution and the numerical one, which is not always acceptable. In particular, the choice of a relatively high wavelet thresholding level undoubtedly affects the accuracy of the numerical simulations.

2.3. Wavelet filter-based modeling

Several SGS models have been developed for closing the SCALES equations (3), both non-localized and localized in physical space, based on both eddy-viscosity and non-eddy-viscosity assumption, e.g. [3,4].

In this work, the deviatoric part of the residual-stress tensor is approximated by the following wavelet-based dynamic Smagorinsky eddy-viscosity model:

$$\tau_{ij}^* \cong -2C_s \Delta^2 |\bar{S}^{>\epsilon}| \bar{S}_{ij}^{>\epsilon}, \quad (5)$$

where $|\bar{S}^{>\epsilon}| = \left(2\bar{S}_{ij}^{>\epsilon} \bar{S}_{ij}^{>\epsilon} \right)^{1/2}$ is the magnitude of the resolved wavelet-filtered rate-of-strain tensor and Δ is the characteristic filter length-scale that is implicitly defined by the WTF level ϵ . The latter parameter should be formally used to properly scale the eddy viscosity. However, it was shown in *a priori* tests for homogeneous isotropic turbulence that $C_s \Delta^2 \sim \epsilon^2$ [17]. Hence,

the filter width Δ can be assumed directly proportional to the threshold ϵ and, for simplicity, the classical formulation can be used.

The SGS dissipation is thus approximated as $\Pi \cong \langle C_S \Delta^2 |\bar{S}^{\epsilon}|^3 \rangle$, where the Smagorinsky model coefficient C_S is determined according to a Germano-like dynamic procedure, by introducing a further test-filtering operation and exploiting a classical least squares method to evaluate the whole group $2C_S \Delta^2$ in (5) as a function of time. All the details about this non-local dynamic modeling procedure for implicit SCALES of homogeneous turbulence can be found in the original work [17].

2.4. Adaptive wavelet collocation method

The AWCM is an adaptive variable-order numerical method for solving problems with localized structures that change their location and scale [18,19]. The method is based on second-generation wavelets [20], which allow the order of the wavelets (and hence of the numerical method) to be varied easily. The grid adaptation is based on wavelet compression and exploits the one-to-one correspondence between grid-points and wavelet coefficients. Wavelet compression is performed in the wavelet space through wavelet coefficient thresholding (1). In a practical calculation, to account for the evolution of the numerical solution over a single time step, the nearest neighbor wavelet coefficients are added, in both position and scale. Since each wavelet corresponds to a single grid point, this procedure allows the grid to automatically follow the flow evolution at each level of resolution. With this adaptation strategy, a solution is obtained on a near optimal collocation grid. The method has a computational complexity $O(N)$, where N is the number of wavelets retained in the calculation.

More specifically, the grid adaptation process for the solution of the filtered Navier–Stokes equations (3) consists of the following steps: (i) knowing the solution $\bar{u}_i^{>\epsilon}$ at current computational grid, say, \mathcal{G}_s^t , the associated wavelet coefficients are computed by means of the forward wavelet transform; (ii) a mask is created for the collocation points that correspond to wavelets with coefficients whose moduli are above the prescribed threshold ϵ ; (iii) the mask is extended by adding grid points corresponding to adjacent wavelets, whose coefficients can potentially become significant at the next time step; (iv) the recursive reconstruction check procedure on the mask is carried out to ensure that all ancestry grid points necessary to perform the forward wavelet transform on the modified mesh $\mathcal{G}_s^{t+\Delta t}$ are present [18].

Regarding the time-integration procedure, a multi-step pressure correction method is employed for the integration of Eq. (3) with the continuity constraint given by Eq. (2) [21]. The resulting Poisson equation is solved using the AWCM elliptic solver developed in [2].

Additionally, it should be mentioned that, as in LES with non-uniform filter width [22–24], there is a commutation error between WTF and differential operators, the effect of which is not considered in this work. However, since the grid adaptation makes use of the adjacent zone, which also includes wavelets with smaller coefficients that can possibly become significant during the single time step, the commutation error is significantly reduced.

3. Explicit wavelet-filtering approach

Instead of exploiting the sole built-in filtering effect of AWCM, alternatively, one can consider two different levels of filtering, by superimposing an additional explicit wavelet filtering operation during the solution process.

3.1. Explicit SCALES equations

According to the explicit filtering approach, WTF at threshold ϵ is explicitly applied upon the non-linear term in the governing equations that are numerically solved at thresholding level $\epsilon_g < \epsilon$. Since the wavelet filter is a projection operator, clearly, it holds $\overline{(\cdot)^{>\epsilon_g}}^{>\epsilon} = \overline{(\cdot)^{>\epsilon}}$, and the momentum equation for the explicitly filtered velocity can be formally written as:

$$\frac{\partial \bar{u}_i^{>\epsilon}}{\partial t} + \frac{\partial \overline{\bar{u}_i^{>\epsilon} \bar{u}_j^{>\epsilon}}^{>\epsilon}}{\partial x_j} = -\frac{1}{\rho} \frac{\partial \bar{p}^{>\epsilon}}{\partial x_i} + \nu \frac{\partial^2 \bar{u}_i^{>\epsilon}}{\partial x_j \partial x_j} - \frac{\partial \bar{\sigma}_{ij}^{>\epsilon}}{\partial x_j}. \quad (6)$$

Here, the unknown stresses to be modeled are defined by

$$\bar{\sigma}_{ij}^{>\epsilon} = \overline{\bar{u}_i \bar{u}_j}^{>\epsilon} - \overline{\bar{u}_i^{>\epsilon} \bar{u}_j^{>\epsilon}}^{>\epsilon} \quad (7)$$

and can be referred to as subfilter-scale (SFS) stresses [8]. When making a comparison with the residual-stresses definition (4), it is apparent that

$$\tau_{ij} = L_{ij} + \bar{\sigma}_{ij}^{>\epsilon}, \quad (8)$$

where $L_{ij} = \overline{\bar{u}_i^{>\epsilon} \bar{u}_j^{>\epsilon}}^{>\epsilon} - \overline{\bar{u}_i^{>\epsilon} \bar{u}_j^{>\epsilon}}$ are the so-called Leonard stresses. While the Leonard stresses are exactly computable in the explicit filtering framework, the SFS stresses account for the effect of filtered-out motions (upon the dynamics of the resolved ones) that can not be however recovered. In fact, definition (7) can be recast in

$$\overline{\sigma_{ij}^{>\epsilon}} = \overline{\overline{u_i^{>\epsilon} u_j^{>\epsilon}}} + \overline{\overline{u_i' u_j^{>\epsilon}}} + \overline{\overline{u_i' u_j'}} \tag{9}$$

directly involving the unknown residual field u_i' .

Along the same line of argument, the energy dissipation associated to the residual stresses can be decomposed as

$$\Pi = \Pi_L + \Pi_{SFS} \tag{10}$$

where the energy dissipation corresponding to the Leonard stresses $\Pi_L \equiv \langle -L_{ij}^* \overline{\overline{S_{ij}^{>\epsilon}}} \rangle$ is directly evaluable, while an approximation for $\Pi_{SFS} \equiv \langle -\overline{\overline{\sigma_{ij}^{>\epsilon}}} \overline{\overline{S_{ij}^{>\epsilon}}} \rangle$ must be provided by the SFS closure model. Clearly, L_{ij}^* and $\overline{\overline{\sigma_{ij}^{>\epsilon}}}$ stand for the anisotropic part of Leonard and SFS stress tensors, respectively.

Note that all terms in the explicit SCALES equations (6) appear as wavelet-filtered quantities at the prescribed threshold ϵ and, thus, effectively correspond to the same desired turbulence resolution. Moreover, the turbulent velocity field to be solved for is still $\overline{u_i^{>\epsilon}}$, while the explicit filtering procedure is just a tool that makes it possible to use a lower WTF level for the numerical grid adaptation. The use of such an approach results in adding extra computational modes beyond the ones that would be strictly necessary to achieve the desired turbulent resolution at level ϵ . However, the computational cost is lower with respect to implicit simulations at level ϵ_g , since the energy cascade in between the two levels is broken by the combined action of explicit filtering and SFS modeling.

It is important to emphasize that in spite of the use of discrete wavelet transform, the wavelet thresholding of the velocity field can be viewed as a multi-level Lagrangian-type spatial filter [4,25]. The Lagrangian nature of the wavelet filtering is achieved by utilizing the adjacent zone mentioned in Section 2.4, which tracks the evolving structures and corresponding filter mask at each level of resolution. Thus, the wavelet-based adaptive LES is different from classical LES with spatially variable filter width, where the governing equations (6) could be not invariant under Galilean transformations [26] and suitable SFS models must be chosen to restore Galilean-invariance, e.g. [27].

Following [28], in order to illustrate the way explicit filtering is actually performed in a practical calculation, a simple Euler time stepping procedure is considered, where the resolved velocity field would be updated according to

$$[\overline{u_i^{>\epsilon}}]^{n+1} = [\overline{u_i^{>\epsilon}}]^n + \Delta t \left[-\frac{\overline{\overline{\partial u_i^{>\epsilon} u_j^{>\epsilon}}}}{\partial x_j} - \frac{1}{\rho} \frac{\partial \overline{\overline{p^{>\epsilon}}}}{\partial x_i} + \nu \frac{\partial^2 \overline{u_i^{>\epsilon}}}{\partial x_j \partial x_j} - \frac{\partial \overline{\overline{\sigma_{ij}^{>\epsilon}}}}{\partial x_j} \right]^n \tag{11}$$

While advancing from time level n to $n + 1$, the non-linear term in the SCALES equations is explicitly filtered at prescribed threshold ϵ , regardless of what thresholding level ϵ_g is actually used by the AWCM numerical procedure. The same holds for the modeled SFS stresses, as reported in the following.

In fact, the grid adaptation process for the solution of the explicitly filtered Navier–Stokes equations (6) consists of the same steps discussed in Section 2.4 for the implicit filtering approach, where the wavelet mask is created based upon the thresholding level ϵ_g . This way, while the numerical resolution is maintained by throwing away those wavelets whose energy is below the prescribed numerical grid level, the desired turbulence resolution is kept by filtering out, step by step, those wavelets whose energy is intermediate between the numerical grid level and the explicit filtering level, which correspond to the lesser resolved motions. Thus, the explicit filtering approach results in using two distinct wavelet masks that identify two different levels of wavelet truncation: the implicit numerical level and the explicit filter level, with the model filtering mask being a subset of the numerical one.

For the sake of clarity, it should be noted that due to the adopted grid adaptation strategy that uses adjacent wavelet collocation points, this picture is not entirely correct. Wavelets with energy below the prescribed level are constantly added to a boundary zone (for both location and scale) in the wavelet collocation space to account for the possible flow evolution during the single time integration step. Since these adjacent wavelets are not filtered-out, according to this formulation, extra smaller scales are actually solved for.

Alternatively, the resolved velocity field could be filtered at threshold ϵ , step-by-step during the simulation, according to

$$[\overline{u_i^{>\epsilon}}]^{n+1} = \overline{[\overline{u_i^{>\epsilon}}]^n + \Delta t \left[-\frac{\partial \overline{u_i^{>\epsilon} u_j^{>\epsilon}}}{\partial x_j} - \frac{1}{\rho} \frac{\partial \overline{p^{>\epsilon}}}{\partial x_i} + \nu \frac{\partial^2 \overline{u_i^{>\epsilon}}}{\partial x_j \partial x_j} - \frac{\partial \overline{\sigma_{ij}^{>\epsilon}}}{\partial x_j} \right]^n} \tag{12}$$

This approach would however result in the correct treatment of the nonlinear term, as well as the SFS stresses, but the other terms would be filtered twice. Theoretically, this is not an issue as WTF is a projection operator, i.e. $\overline{\overline{u_i^{>\epsilon}}} = \overline{u_i^{>\epsilon}}$, but, practically, wavelets in the adjacent zone would be wiped-out, leading to extra dissipation of resolved kinetic-energy. The existence of this extra dissipation has been verified in practical simulations, as demonstrated by the results reported in this paper.

3.2. Subfilter-scale model

The closure models used in the past for implicit SCALES of turbulent flows can be consistently revised in order to be applied in conjunction with the new explicit filtering procedure.

In this work, following the eddy-viscosity dynamic Smagorinsky modeling approach proposed in [17], the deviatoric part of the SFS turbulent stress tensor is approximated as

$$\overline{\sigma_{ij}^{>\epsilon}} \cong -2C_s \Delta^2 \overline{|\widehat{S}^{>\epsilon}| \widehat{S}_{ij}^{>\epsilon}}. \tag{13}$$

The Smagorinsky modeling coefficient C_s is determined as a function of time according to a dynamic procedure, by introducing a further test-filtering operation with a larger characteristic filter width $\widehat{\Delta} > \Delta$. Two different procedures can be used for test-filtering, by either constructing a local lowpass filter on the adaptive mesh or using the WTF procedure with a larger threshold. A local low-pass discrete test-filter can be constructed by exploiting a number of adjacent grid points that ensure the proper filter width and positive filter weights [3]. As an alternative, WTF at larger thresholding level $\widehat{\epsilon}$ can be used as test-filter [17], thus implicitly defining the characteristic filter width $\widehat{\Delta}$. Due to its better performance, only the results for the latter test filtering procedure with doubled thresholding level ($\widehat{\epsilon} = 2\epsilon$) are considered in this work.

Formally denoting the test-filtered resolved velocity field as $\widehat{u_i}^{>\epsilon}$, the SFS residual-stress tensor at the test-filter level is defined as

$$\widehat{T_{ij}^{>\epsilon}} = \widehat{u_i u_j}^{>\epsilon} - \overline{\widehat{u_i}^{>\epsilon} \widehat{u_j}^{>\epsilon}}. \tag{14}$$

By filtering Eq. (7) at the test-filter level and combining it with (14), the following modified Germano identity is obtained:

$$\widehat{T_{ij}^{>\epsilon}} - \widehat{\sigma_{ij}^{>\epsilon}} = \overline{\widehat{u_i}^{>\epsilon} \widehat{u_j}^{>\epsilon}}^{>\epsilon} - \overline{\widehat{u_i}^{>\epsilon} \widehat{u_j}^{>\epsilon}} \equiv \widehat{\mathcal{L}_{ij}^{>\epsilon}}. \tag{15}$$

Given the test-filter definition, the above stresses are directly computable from the resolved velocity field and can be exploited to dynamically evaluate the unknown model coefficient as follows.

Assuming that the same Smagorinsky eddy-viscosity model, with the same model coefficient, can be used for the stress tensor at the test level, the deviatoric part of $\widehat{T_{ij}^{>\epsilon}}$ is approximated, analogously to (13), as

$$\widehat{T_{ij}^{>\epsilon*}} \cong -2C_s \widehat{\Delta}^2 \overline{|\widehat{S}^{>\epsilon}| \widehat{S}_{ij}^{>\epsilon}}, \tag{16}$$

where $\widehat{S}_{ij}^{>\epsilon} = 1/2(\partial \widehat{u_i}^{>\epsilon} / \partial x_j + \partial \widehat{u_j}^{>\epsilon} / \partial x_i)$ is the test-filtered rate-of-strain tensor and $|\widehat{S}^{>\epsilon}| = (2\widehat{S}_{ij}^{>\epsilon} \widehat{S}_{ij}^{>\epsilon})^{1/2}$ represents its magnitude.

Exploiting the modeling approximations (13) and (16), Eq. (15) becomes

$$2C_s \Delta^2 \overline{|\widehat{S}^{>\epsilon}| \widehat{S}_{ij}^{>\epsilon}}^{>\epsilon} - 2C_s \widehat{\Delta}^2 \overline{|\widehat{S}^{>\epsilon}| \widehat{S}_{ij}^{>\epsilon}} = \widehat{\mathcal{L}_{ij}^{>\epsilon*}}, \tag{17}$$

where $\widehat{\mathcal{L}_{ij}^{>\epsilon*}}$ stands for the deviatoric part of the known stresses tensor $\widehat{\mathcal{L}_{ij}^{>\epsilon}}$. A least square solution to (17) leads to the following equation for determining the unknown Smagorinsky model coefficient:

$$2C_s \Delta^2 = \frac{\widehat{\mathcal{L}_{ij}^{>\epsilon*}} \widehat{M_{ij}^{>\epsilon}}}{\widehat{M_{hk}^{>\epsilon}} \widehat{M_{hk}^{>\epsilon}}}, \tag{18}$$

with

$$\widehat{M_{ij}^{>\epsilon}} \equiv \overline{|\widehat{S}^{>\epsilon}| \widehat{S}_{ij}^{>\epsilon}}^{>\epsilon} - \alpha^2 \overline{|\widehat{S}^{>\epsilon}| \widehat{S}_{ij}^{>\epsilon}}, \tag{19}$$

where $\alpha \equiv \widehat{\Delta} / \Delta$ is the test-filter to explicit filter width ratio. When using the WTF procedure for test-filtering, this parameter is explicitly defined by the ratio of the test-filtering and explicit-filtering thresholds, i.e. $\alpha \equiv \widehat{\epsilon} / \epsilon$. Given the existing direct proportionality between Δ and ϵ , the test-filter to explicit filter width ratio $\alpha = 2$ is assumed for the numerical experiments presented in the following.

Finally, as usually done for dynamic LES of homogeneous turbulence, both the numerator and denominator at the right-hand side of Eq. (18) are volume-averaged in order to have stable numerical solutions. This way, the whole group $2C_s \Delta^2$ is determined, as a function of time only, according to

$$2C_s \Delta^2 = \frac{\langle \widehat{\mathcal{L}_{ij}^{>\epsilon*}} \widehat{M_{ij}^{>\epsilon}} \rangle}{\langle \widehat{M_{hk}^{>\epsilon}} \widehat{M_{hk}^{>\epsilon}} \rangle}, \tag{20}$$

which actually leads to a non-local modeling procedure.

4. Numerical experiments

In order to carry out some numerical experiments, the simulation of decaying homogeneous incompressible turbulence is considered, which also allows the comparison with previous implicit SCALES studies [3,4]. The initial condition for the velocity field is provided by wavelet-filtering a statistically steady pseudo-spectral DNS solution at $Re_\lambda \cong 120$. The spectral direct solution is obtained by solving the unfiltered Navier–Stokes equations, supplied with the random forcing scheme of Eswaran and Pope [29], with 384^3 Fourier modes [15]. The same pseudo-spectral code, with the same resolution, is used to produce a reference DNS solution for the decaying case (for discussion SDNS). The moderate initial Reynolds-number is however sufficiently high to show a clear inertial range in the energy spectrum.

Although the AWCM procedure used for numerically solving the SCALES equations is based on a sixth-order finite difference discretization, the smallest resolved scales are not accurately represented due to polynomial nature of wavelet approximation. Thus, in order to approximately retain the same degree of numerical accuracy, the maximum spatial resolution is increased with respect to SDNS. In practice, seven nested wavelet collocation grids, with effective resolutions ranging from 8^3 to 512^3 , are employed in the simulations. However, depending on the actual thresholding level that is used, only a subset of available wavelets identified by the explicit filter mask are used. It is worth noting that the effective number of wavelets that are involved is typically very low with respect to the available maximum value, owing to the high compression property of the wavelet-based methods discussed in Section 2.1. In addition, due to the decaying nature of the turbulent flow under consideration, a great number of wavelets is only required during the initial period, with a gradual decrease of the necessary level of wavelet resolution as turbulence decays.

In terms of computational cost, the comparison with the pseudo-spectral solution is not straightforward, as grid-compression is not the only factor to be considered. On one hand, it is necessary to look at the cost associated with the use of the adaptive multi-resolution wavelet methodology, which is per grid-point approximately three to five times greater than the one of the corresponding non-adaptive finite difference method. On the other hand, the AWCM procedure provides huge memory savings that allow higher resolution numerical simulations to be performed, for given available computational resources. A detailed comparison between wavelet-based and Fourier decomposition of homogeneous turbulence can be found in [1,10].

4.1. Implicitly filtered solutions

When explicit filtering is not applied during the calculations, the built-in physical filtering effect induced by the AWCM procedure is used. In this case, the turbulence resolution is dictated by the numerical one that corresponds to have $\epsilon = \epsilon_g$. Three different implicit SCALES solutions are obtained for $\epsilon_g = 0.35, 0.30$ and 0.20 , supplied with the dynamic eddy-viscosity model reviewed in Section 2.3.

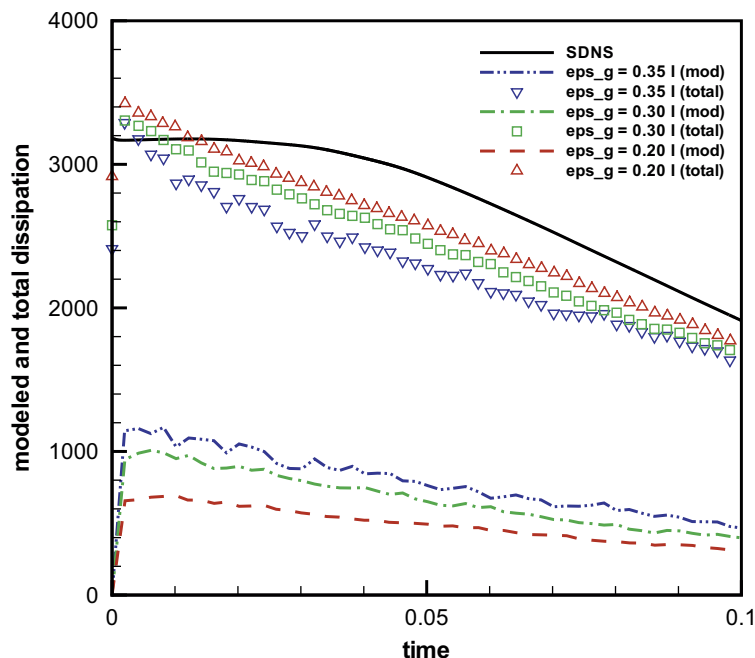


Fig. 1. Modeled and total (resolved plus modeled) dissipation for implicit SCALES with different filtering thresholds.

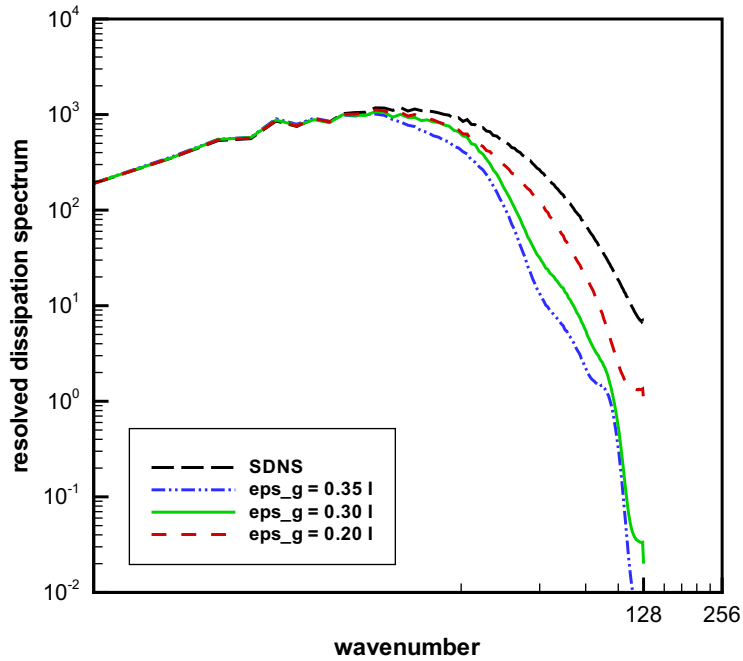


Fig. 2. Resolved dissipation spectra at $t = 0.03$ for implicit SCALES with different filtering thresholds.

By decreasing the wavelet thresholding level, the implicit SCALES solution unavoidably tends toward the direct solution of the unfiltered equations. That is clearly seen by making a comparison with reference (unfiltered) SDNS, for instance, in terms of resolved kinetic-energy dissipation. The time history of the volume-average of this variable is reported in Fig. 1, while the enstrophy spectra at a given time instant, which is $t = 0.03$, are illustrated in Fig. 2. For all the implicit SCALES experiments, given the relatively high value of WTF level that is used, the finest wavelet collocation grid is actually not involved and the maximum adaptive resolution corresponds to 256^3 wavelets. The number of wavelets retained in the calculation, which is not illustrated for brevity, clearly increases with the resolution.

As seen by inspection of both figures, with finer turbulence resolution, which corresponds to lower thresholding level, the resolved dissipation increases and the modeled one decreases, while the total dissipation (resolved plus modeled) tends toward the SDNS viscous dissipation. It should be noted that the discrepancy in the total dissipation for different thresholding levels is attributed to the additional dissipation of kinetic-energy due to discarding of wavelet coefficients during the grid adaptation process, which is not taken into account by the modeling procedure, since grid adaptation occurs at the end of the time step integration.

In fact, for low thresholds, the coherent vortex simulation (CVS) regime is approached, where the SGS dissipation does not need to be modeled [30]. In this case, the net effect of unresolved eddies upon the dynamics of resolved ones corresponds to white Gaussian noise and can be thus neglected, while however preserving the statistical predictability of the turbulent flow field [12]. Finally, for even lower thresholds, the wavelet-based DNS regime would be achieved, where all the relevant turbulent scales are fully resolved.

4.2. Explicitly filtered solutions

In order to illustrate the results for wavelet-based adaptive LES with explicit filtering, a sequence of solutions with different numerical accuracy are presented, for a given desired turbulence resolution that corresponds to $\epsilon = 0.35$. The different numerical solutions are obtained with thresholding level ranging from $\epsilon_g = 0.30$ down to 0.05. As discussed in Section 3.1, WTF at threshold ϵ is explicitly applied upon the non-linear term, step-by-step during the calculations, while the wavelet collocation grid is adapted by applying the same wavelet-based filter, but at threshold ϵ_g .

The different simulations are conducted for the initial period of decay, for a time interval that allows to demonstrate the convergence towards a grid-independent solution. This short time is however sufficient to have a significant decay for the turbulent kinetic-energy that becomes about 20% of the initial value.

In presenting the results, the reference SDNS solution is wavelet-filtered at threshold ϵ in order to have a meaningful comparison with adaptive LES solutions. The wavelet-filtered DNS stands for the ideal solution that explicit SCALES would yield in absence of any modeling error and for “infinite” numerical accuracy.

The time histories of volume-averaged resolved kinetic-energy ($\frac{1}{2}\overline{u_i^2}^{\epsilon-\epsilon}$) and resolved viscous dissipation ($\langle 2\nu S_{ij}^{\epsilon-\epsilon} S_{ij}^{\epsilon-\epsilon} \rangle$) are reported in Figs. 3 and 4, respectively, for the different numerical thresholds. Furthermore, in order to examine the same

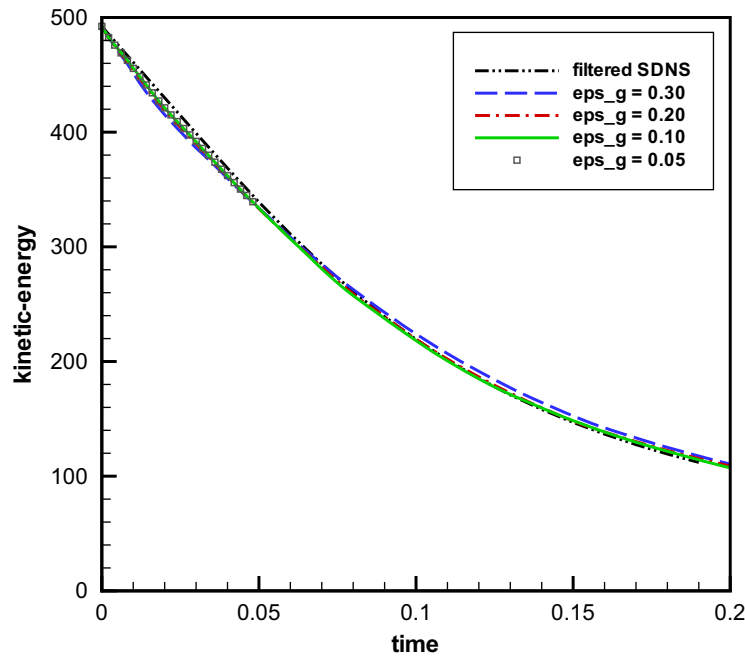


Fig. 3. Resolved kinetic-energy for explicit SCALES with different numerical thresholds.

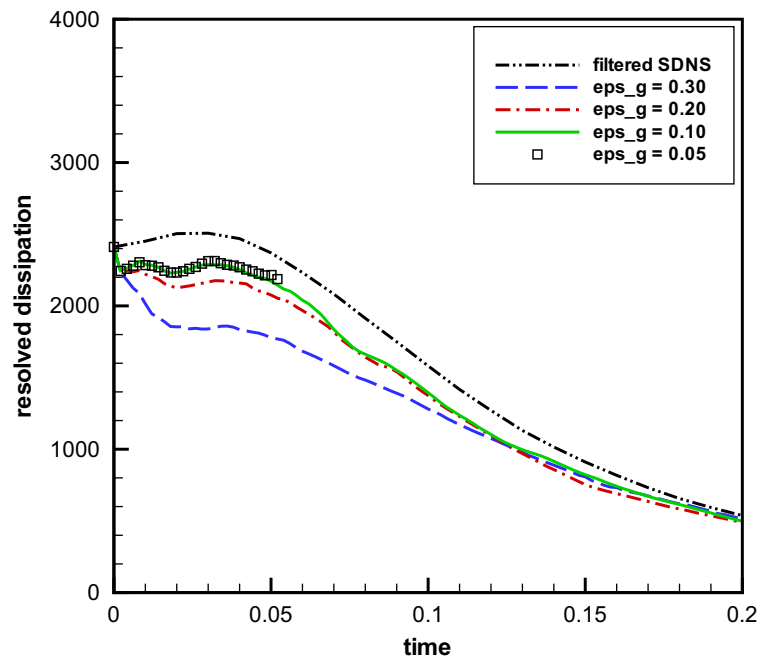


Fig. 4. Resolved viscous dissipation for explicit SCALES with different numerical thresholds.

solutions in wavenumber space, the instantaneous spectra of resolved energy and resolved enstrophy are illustrated in Figs. 5 and 6, respectively, at the same time instant chosen for the implicit solutions, which is $t = 0.03$. In this case, for the smallest values of ϵ_g , the finest wavelet collocation grid is actually involved and the maximum adaptive resolution corresponds to 512^3 wavelets.

By inspection of these results, it clearly appears that, with the progressive improvement of the numerical accuracy, viz., for decreasing numerical thresholding level ϵ_g , the SCALES solution does approach a grid-independent solution, tending to-

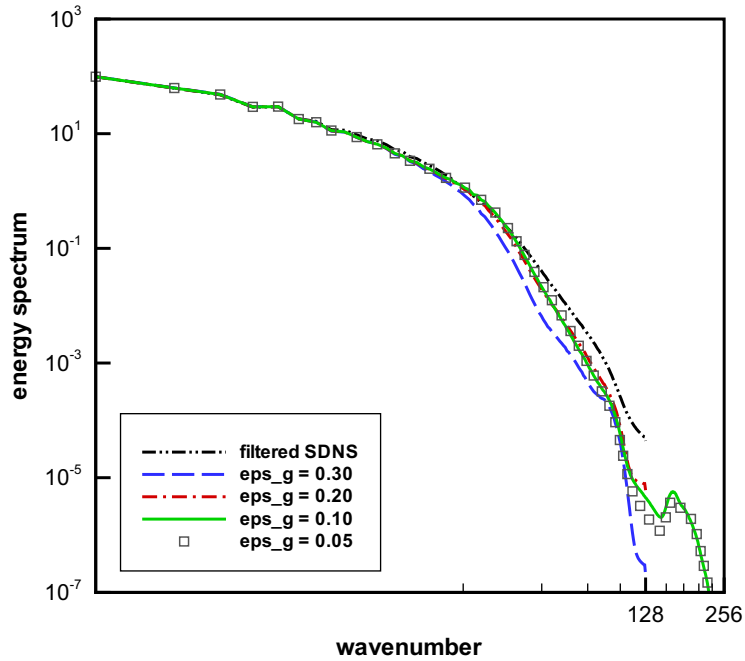


Fig. 5. Kinetic-energy spectra at $t = 0.03$ for explicit SCALES with different numerical thresholds.

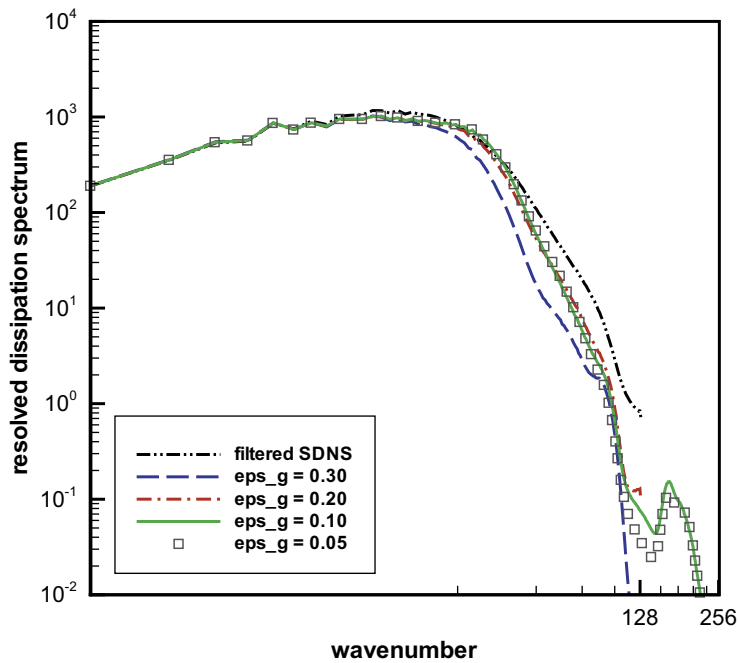


Fig. 6. Resolved dissipation spectra at $t = 0.03$ for explicit SCALES with different numerical thresholds.

ward the filtered SDNS. The converged solution can be thought as representing the ideal evolution of the wavelet-filtered velocity field corresponding to the more energetic coherent turbulent flow eddies (as defined by the prescribed explicit WTF level ϵ). The discrepancy between converged solution and filtered SDNS is to be attributed to the unavoidable approximation induced by the adopted SFS model.

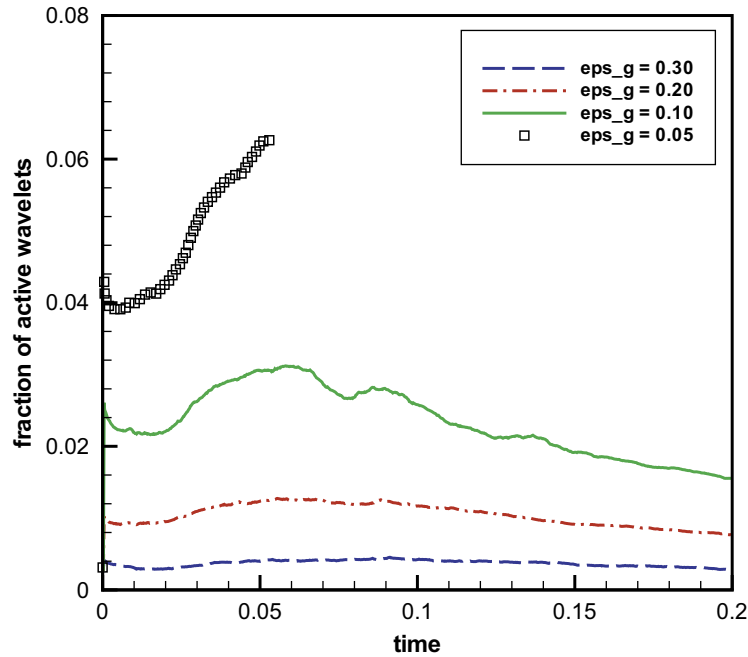


Fig. 7. Fraction of retained wavelets for explicit SCALES with different numerical thresholds.

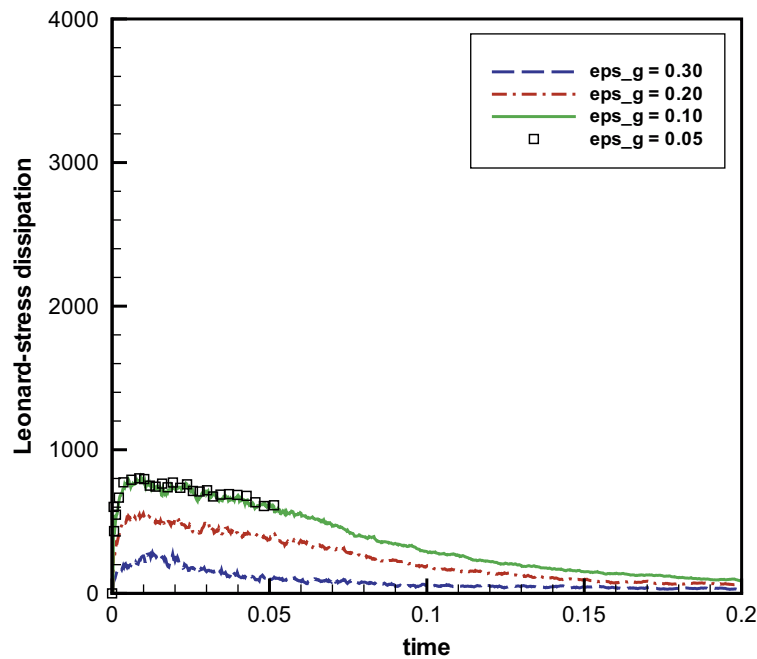


Fig. 8. Leonard-stress dissipation for explicit SCALES with different numerical thresholds.

As discussed in Section 3.1, the use of adjacent wavelets for grid-adaptation leads to the creation of extra scales at level lower than the prescribed one. This is clearly seen by inspection of energy spectra and, more evidently, enstrophy spectra, which are slightly higher with respect to filtered SDNS at small resolved scales.

Obviously, the number of wavelets retained in the calculation increases with the decrease of ϵ_g , as shown in Fig. 7. For the smallest value investigated that is $\epsilon_g = 0.05$, the maximum number of active wavelets is about 6% of the total available wavelets. However, in order to practically achieve a grid-independent solution, it is sufficient to exploit less than 3% of the available wavelets, which corresponds to fix $\epsilon_g = 0.10$.

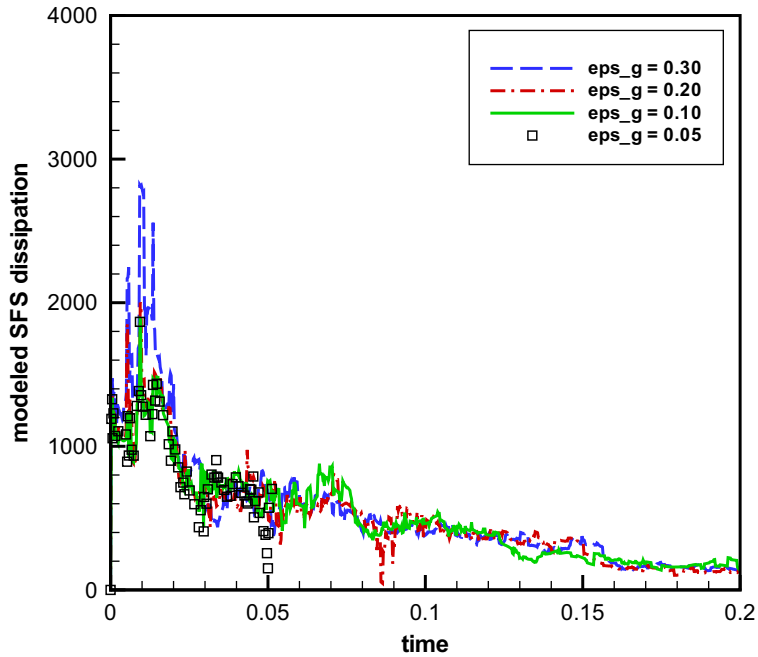


Fig. 9. Modeled SFS dissipation for explicit SCALES with different numerical thresholds.

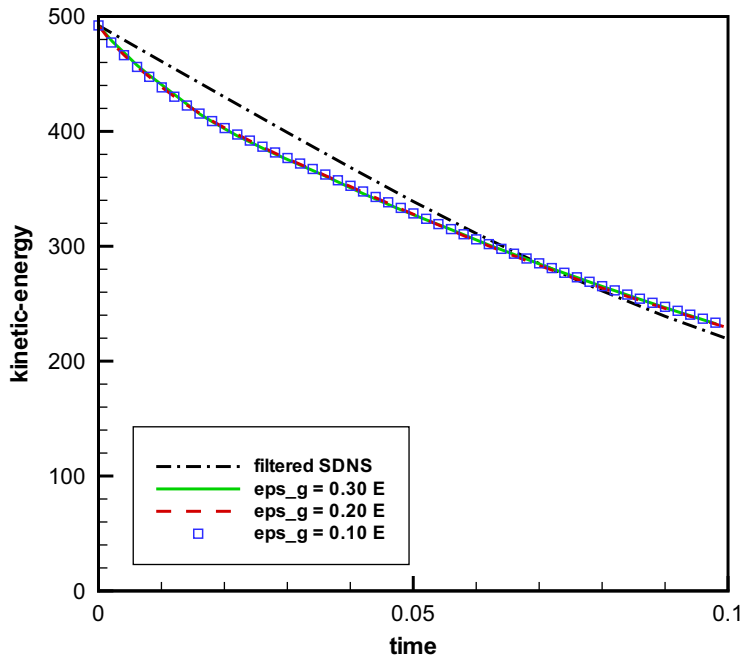


Fig. 10. Resolved kinetic-energy for explicit SCALES with different numerical thresholds and explicit filtering of velocity field.

As to energy dissipation associated to the residual stresses Π , the two different contributions, corresponding to the known Leonard stresses, Π_L , and the modeled SFS ones, Π_{SFS} , are depicted in Figs. 8 and 9, respectively. By refining the wavelet collocation numerical grid, a better evaluation of the Leonard-stress dissipation is obtained. On the contrary, the magnitude of the modeled SFS dissipation appears not to depend on the grid resolution. Hence, the modeling error associated with the use of the eddy-viscosity-based approximation (13) remains constant, regardless of the numerical accuracy of the solu-

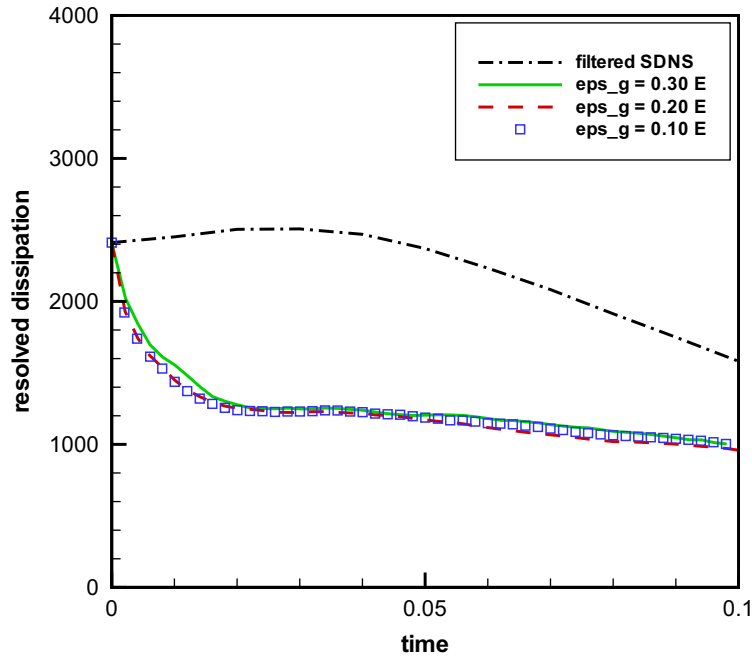


Fig. 11. Resolved viscous dissipation for explicit SCALES with different numerical thresholds and explicit filtering of velocity field.

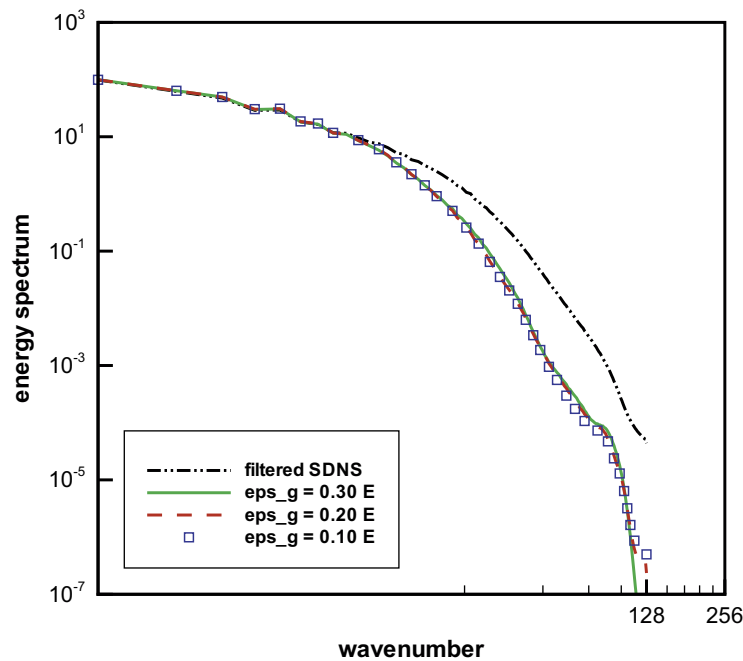


Fig. 12. Kinetic-energy spectra at $t = 0.03$ for explicit SCALES with different numerical thresholds and explicit filtering of velocity field.

tion. This is mainly due to the fact that the modeling procedure employs an explicit filtering operation at level $\epsilon > \epsilon_g$, which makes the modeled SFS stresses practically insensitive to numerical errors.

It is worth noting that, for any practical purpose, the experiment corresponding to $\epsilon_g = 0.10$ can be considered as providing a grid-converged solution that matches the prescribed turbulence resolution. Turbulence statistics and energy/enstrophy spectra for $\epsilon_g = 0.10$ and 0.05 are shown to practically collapse. For this reason, in order to save computational resources, the calculation with the smallest numerical threshold used has been conducted for a shorter time interval.

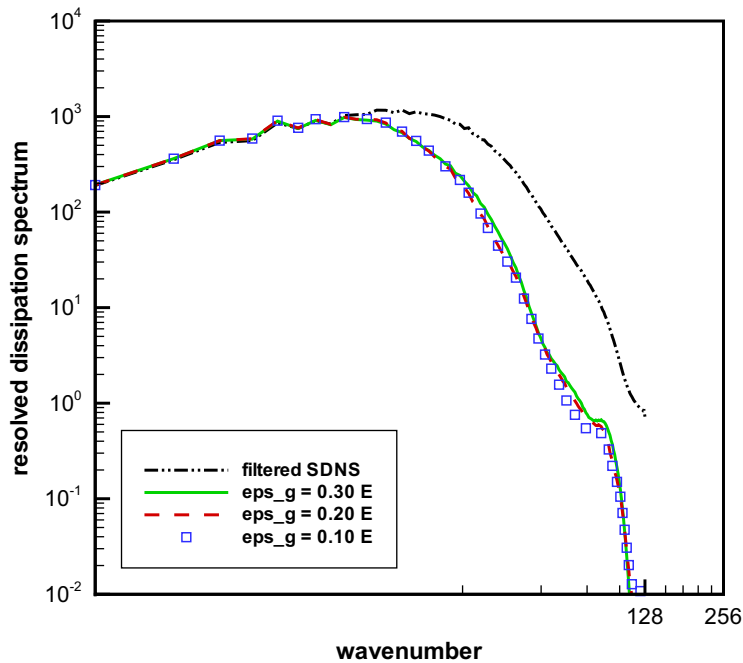


Fig. 13. Resolved dissipation spectra at $t = 0.03$ for explicit SCALES with different numerical thresholds and explicit filtering of velocity field.

Finally, in order to make a useful comparison, additional tests, where the adaptive LES solutions are obtained by explicitly filtering the velocity field at each time-step during the calculation, have been considered. The evolutions of kinetic-energy and resolved viscous dissipation are reported in Figs. 10 and 11, respectively, while the energy and enstrophy spectra at the same time instant of previous figures are depicted in Figs. 12 and 13, respectively. In this case, the use of smaller numerical thresholds ϵ_g does not help since, as clearly demonstrated in the figures, increasing the numerical accuracy has a very negligible effect upon the solution.

This approach has some connection with those LES methods that employ a secondary filtering process as a regularization step to obtain a stable numerical solution. By comparing the solutions presented in Figs. 12 and 13 to those illustrated in Figs. 5 and 6, it is apparent how this procedure is impractical for wavelet-based adaptive LES. In fact, the adjacent zone involving wavelet collocation points that can possibly become significant during the time integration step is swept out, because resolved wavelets with smaller coefficient are removed step-by-step by the explicit filtering operation, which directly acts upon the velocity field. For the same reason, even the dynamic modeling procedure by itself does not work properly. Thus, the flow evolution is completely altered and the actual resolution is dominated by the explicit filtering process.

5. Concluding remarks

In this work, the wavelet-based adaptive LES method is applied with superimposed explicit wavelet filtering. The application of additional filtering to the nonlinear term in the governing equations allows for a clear separation between resolved motions and unresolved ones, while controlling the truncation error associated to the use of numerical finite differences. Grid-independent solutions are achieved by refining the wavelet collocation grid, while maintaining the prescribed wavelet thresholding level that corresponds to the desired turbulence resolution.

This study sheds new insights on the analysis of the quality of wavelet-filtered solutions with respect to ideal grid-independent calculations, thus enhancing our knowledge about the strong interactions between filtering, modeling, and numerical errors in wavelet-based LES. Also, the explicit filtering formulation allows for a deeper examination of the performance of the modeling procedure and tighter control of the numerical error. In particular, as the failure of grid-independent explicitly filtered solutions in matching wavelet-filtered DNS can be attributed to residual-stress modeling errors, this analysis can help in the development of more efficient closure models.

In view of these results, pure “physical” SCALES, where the numerical errors are negligible, can be performed with a suitable value of the explicit filter to numerical-filter threshold ratio. However, in practical applications, where the computational cost must be taken into account, the optimal value of this ratio is expected to correspond to low but non-negligible numerical errors.

Although the wavelet-based adaptive LES methodology is not mature enough for complex geometry flow simulations, substantial progress is being made towards achieving this goal by exploiting the volume-penalization technique, which

works extremely well with the adaptive wavelet collocation method. The present explicit-filtering approach, along with the recent development of the parallel wavelet-based solver, represents a crucial step in this ongoing process.

Acknowledgments

This work was supported by the Department of Energy (DOE) under Grant No. DE-FG02-07ER64468 and the National Science Foundation (NSF) under Grant Nos. CBET-0756046 and CBET-123650. In addition, G. De Stefano was partially supported by a grant from the Italian Ministry of Foreign Affairs (Selected Joint Mobility Project for the Exchange of Researchers between Italy and United States of America). These supports are gratefully acknowledged.

References

- [1] D.E. Goldstein, O.V. Vasilyev, Stochastic coherent adaptive large eddy simulation method, *Phys. Fluids* 16 (7) (2004) 2497–2513.
- [2] O.V. Vasilyev, N.K.R. Kevlahan, An adaptive multilevel wavelet collocation method for elliptic problems, *J. Comput. Phys.* 206 (2) (2005) 412–431.
- [3] G. De Stefano, O.V. Vasilyev, D.E. Goldstein, Localized dynamic kinetic energy-based models for stochastic coherent adaptive large eddy simulation, *Phys. Fluids* 20 (4) (2008) 045102.1–045102.14.
- [4] O.V. Vasilyev, G. De Stefano, D.E. Goldstein, N.K.R. Kevlahan, Lagrangian dynamic SGS model for stochastic coherent adaptive large eddy simulation, *J. Turbul.* 9 (11) (2008) 1–14.
- [5] S. Pope, Ten questions concerning the large-eddy simulation of turbulent flows, *New J. Phys.* 6 (2004) 1–24.
- [6] G.S. Winkelmans, A.A. Wray, O.V. Vasilyev, H. Jeanmart, Explicit-filtering large-eddy simulation using the tensor-diffusivity model supplemented by a dynamic Smagorinsky term, *Phys. Fluids* 13 (5) (2001) 1385–1403.
- [7] J. Gullbrand, F.K. Chow, The effect of numerical errors and turbulence models in large-eddy simulations of channel flow with and without explicit filtering, *J. Fluid Mech.* 495 (2003) 323–341.
- [8] S.T. Bose, P. Moin, D. You, Grid-independent large-eddy simulation using explicit filtering, *Phys. Fluids* 22 (10) (2010) 105103.1–105103.11.
- [9] M. Farge, G. Pellegrino, K. Schneider, Coherent vortex extraction in 3D turbulent flows using orthogonal wavelets, *Phys. Rev. Lett.* 87 (5) (2001) 054501.
- [10] M. Farge, K. Schneider, G. Pellegrino, A. Wray, R. Rogallo, Coherent vortex extraction in three-dimensional homogeneous turbulence: comparison between CVS-wavelet and POD-fourier decompositions, *Phys. Fluids* 15 (10) (2003) 2886–2896.
- [11] K. Schneider, O.V. Vasilyev, Wavelet methods in computational fluid dynamics, *Ann. Rev. Fluid Mech.* 42 (2010) 473–503.
- [12] N. Okamoto, K. Yoshimatsu, K. Schneider, M. Farge, Y. Kaneda, Coherent vorticity simulation of three-dimensional forced homogeneous isotropic turbulence, *Multiscale Model. Simul.* 9 (2011) 1144–1161.
- [13] P. Sagaut, S. Deck, M. Terracol, *Multiscale and Multiresolution Approaches in Turbulence*, Imperial College Press, 2006.
- [14] D. L. Donoho, *Interpolating wavelet transforms*, Tech. Rep. 408, Department of Statistics, Stanford University, 1992.
- [15] G. De Stefano, D.E. Goldstein, O.V. Vasilyev, On the role of sub-grid scale coherent modes in large eddy simulation, *J. Fluid Mech.* 525 (2005) 263–274.
- [16] G. De Stefano, O.V. Vasilyev, Stochastic coherent adaptive large eddy simulation of forced isotropic turbulence, *J. Fluid Mech.* 646 (2010) 453–470.
- [17] D.E. Goldstein, O.V. Vasilyev, N.K.R. Kevlahan, CVS and SCALES simulation of 3D isotropic turbulence, *J. Turbul.* 6 (37) (2005) 1–20.
- [18] O.V. Vasilyev, C. Bowman, Second generation wavelet collocation method for the solution of partial differential equations, *J. Comput. Phys.* 165 (2000) 660–693.
- [19] O.V. Vasilyev, Solving multi-dimensional evolution problems with localized structures using second generation wavelets, *Int. J. Comput. Fluid Dynam.* 17 (2) (2003) 151–168. Special issue on High-resolution methods in Computational Fluid Dynamics.
- [20] W. Sweldens, The lifting scheme: A construction of second generation wavelets, *SIAM J. Math. Anal.* 29 (2) (1998) 511–546.
- [21] N.K.R. Kevlahan, O.V. Vasilyev, An adaptive wavelet collocation method for fluid-structure interaction at high Reynolds numbers, *SIAM J. Sci. Comput.* 26 (6) (2005) 1894–1915.
- [22] O.V. Vasilyev, T.S. Lund, P. Moin, A general class of commutative filters for LES in complex geometries, *J. Comput. Phys.* 146 (1998) 105–123.
- [23] A.L. Marsden, O.V. Vasilyev, P. Moin, Construction of commutative filters for LES on unstructured meshes, *J. Comput. Phys.* 175 (2002) 584–603.
- [24] A. Haselbacher, O.V. Vasilyev, Commutative discrete filtering on unstructured grids based on least-squares techniques, *J. Comput. Phys.* 187 (1) (2003) 197–211.
- [25] C. Meneveau, T.S. Lund, W.H. Cabot, A Lagrangian dynamic subgrid-scale model of turbulence, *J. Fluid Mech.* 319 (1996) 353–385.
- [26] C.G. Speziale, Galilean invariance of subgrid-scale stress models in large-eddy simulation of turbulence, *J. Fluid Mech.* 156 (1985) 55–62.
- [27] J. Gullbrand, Grid-independent large-eddy simulation in turbulent channel flow using three-dimensional explicit filtering, *Center for Turbulence Research Annual Research Briefs*, 2003, pp. 331–342.
- [28] T.S. Lund, The use of explicit filters in large eddy simulation, *Comput. Math. Appl.* 46 (2003) 603–616.
- [29] V. Eswaran, S.B. Pope, Direct numerical simulations of the turbulent mixing of a passive scalar, *Phys. Fluids* 31 (1988) 506–520.
- [30] M. Farge, K. Schneider, N.K.R. Kevlahan, Non-Gaussianity and coherent vortex simulation for two-dimensional turbulence using an adaptive orthogonal wavelet basis, *Phys. Fluids* 11 (8) (1999) 2187–2201.